AD_____

Award Number: W81XWH-07-1-0065

TITLE: Effects of radiation on proteasome function in prostate cancer cells

PRINCIPAL INVESTIGATOR: Frank Pajonk

CONTRACTING ORGANIZATION: University of California
Los Angeles, CA 90024

REPORT DATE: February 2008

TYPE OF REPORT: Annual Summary

PREPARED FOR: U.S. Army Medical Research and Materiel Command
Fort Detrick, Maryland 21702-5012

REPORT DOCUMENTATION PAGE

Form Approved
OMB No. 0704-0188

1. REPORT DATE	2. REPORT TYPE	3. DATES COVERED
14-02-2008	Annual Summary	15 JAN 2007 - 14 JAN 2008

4. TITLE AND SUBTITLE
Effects of radiation on proteasome function in prostate cancer cells

5a. CONTRACT NUMBER

5b. GRANT NUMBER
W81XWH-07-1-0065

5c. PROGRAM ELEMENT NUMBER

6. AUTHOR(S)
Frank Pajonk

Email: fpajonk@mednet.ucla.edu

5d. PROJECT NUMBER

5e. TASK NUMBER

5f. WORK UNIT NUMBER

7. PERFORMING ORGANIZATION NAME(S) AND ADDRESS(ES)

University of California
Los Angeles, CA 90024

8. PERFORMING ORGANIZATION REPORT NUMBER

9. SPONSORING / MONITORING AGENCY NAME(S) AND ADDRESS(ES)
U.S. Army Medical Research and Materiel Command
Fort Detrick, Maryland 21702-5012

10. SPONSOR/MONITOR'S ACRONYM(S)

11. SPONSOR/MONITOR'S REPORT NUMBER(S)

12. DISTRIBUTION / AVAILABILITY STATEMENT
Approved for Public Release; Distribution Unlimited

13. SUPPLEMENTARY NOTES

14. ABSTRACT

None Listed.

15. SUBJECT TERMS

None listed.

16. SECURITY CLASSIFICATION OF:			17. LIMITATION OF ABSTRACT	18. NUMBER OF PAGES	19a. NAME OF RESPONSIBLE PERSON
a. REPORT	b. ABSTRACT	c. THIS PAGE			USAMRMC
U	U	U	UU	11	19b. TELEPHONE NUMBER *(include area code)*

Table of Contents

Introduction

The proposed research in this proposal is based on our observation that the 26S proteasome is a direct target of radiation.

In our initial statement of work, we proposed experiments investigating association and release of PIPs from the 26S proteasome as well as to study structural changes of the proteasome in response to radiation. We further intended to clarify to which extend proteasome subunit expression is regulated at the transcriptional, and posttranslational level in response to ionizing radiation. The final goal is to investigate these changes using cutting edge proteomic tools to identify the radiation target within the proteasome in prostate cancer. The aims are unaltered from the original submission.

Body

Our initial reports stated immediate inhibition of proteasome function within minutes after exposure to radiation. Given the slow turnover of this protease it appeared very unlikely that this inhibition resulted

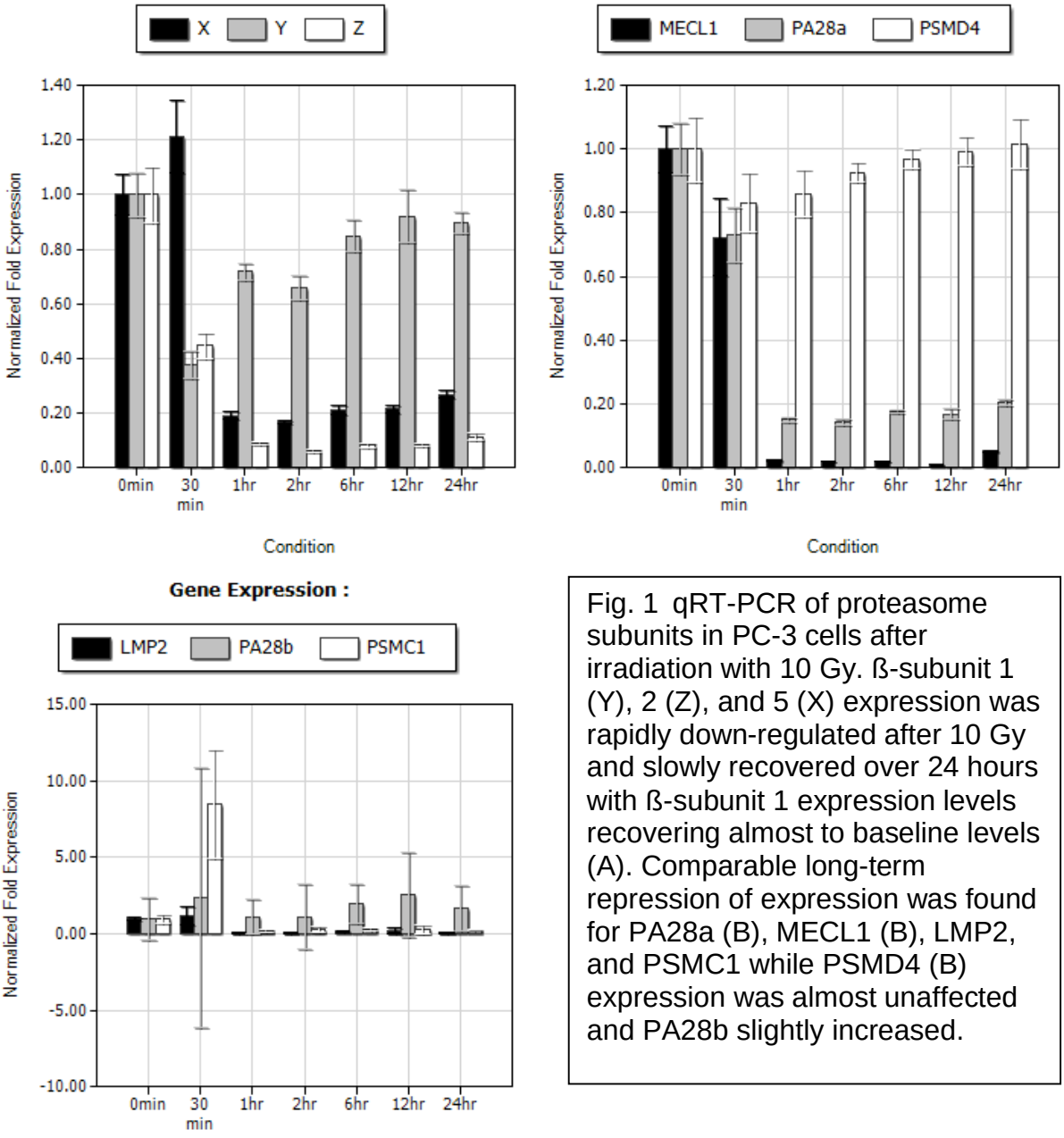

Fig. 1 qRT-PCR of proteasome subunits in PC-3 cells after irradiation with 10 Gy. ß-subunit 1 (Y), 2 (Z), and 5 (X) expression was rapidly down-regulated after 10 Gy and slowly recovered over 24 hours with ß-subunit 1 expression levels recovering almost to baseline levels (A). Comparable long-term repression of expression was found for PA28a (B), MECL1 (B), LMP2, and PSMC1 while PSMD4 (B) expression was almost unaffected and PA28b slightly increased.

from inhibition of proteasome subunit expression. However, in an attempt to exclude this possibility and to investigate a possible up-regulation of subunit expression as a mechanism of recovery, we performed quantitative real-time RT-PCR using PC-3 cells exposed to a single dose of 0 or 10 Gy. ß-type subunit 1 (Y), 2 (Z), and 5 (X) expression was rapidly down-regulated after 10 Gy and slowly recovered over 24 hours with ß-subunit 1 expression levels recovering almost to baseline levels (A). Comparable long-term repression of expression was found for PA28a (B), MECL1 (B), LMP2, and PSMC1 while PSMD4 (B) expression was almost unaffected and PA28b slightly increased (Figure 1) Taken together, this data suggest that, even though decreased subunit expression may not explain the immediate drop in proteasome function, it may indicate why proteasome function after radiation remains low for several hours after irradiation.

Our group had previously shown that irradiation caused an increase in ATPase activity in fractions containing the 26S proteaome.

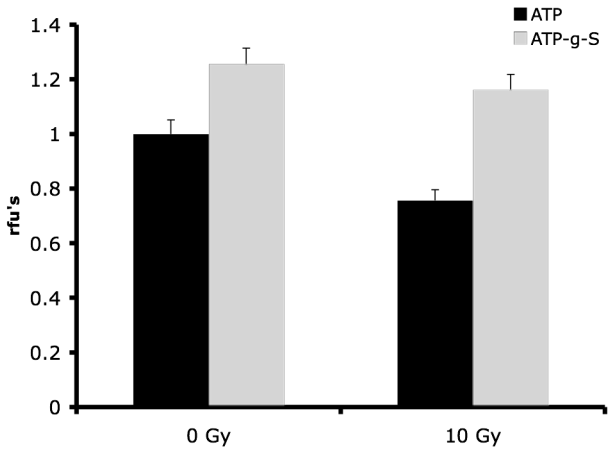

Fig. 2 Radiation-induced proteasome inhibition was inhibited by ATP-g-S. PC3 cell extracts were incubated with 3mM ATP or 2mM non-hyrdolysable ATP-g-S. Irradiation (10Gy) ha no effect in the presence of ATP-g-S indicating the requirement for ATP hydrolysis for radiation induced inhibition of proteasome function

This led us to ask if it was dependent on ATP hydrolysis. The nonhydrolysable form of ATP, ATPgS did not allow radiation-induced proteasome inhibition, although appeared to maintain 26S structure, as expected. In fact, activity was slightly elevated, perhaps because ATP-dependent proteasome disassembly during the assay did not occur (figure 2).

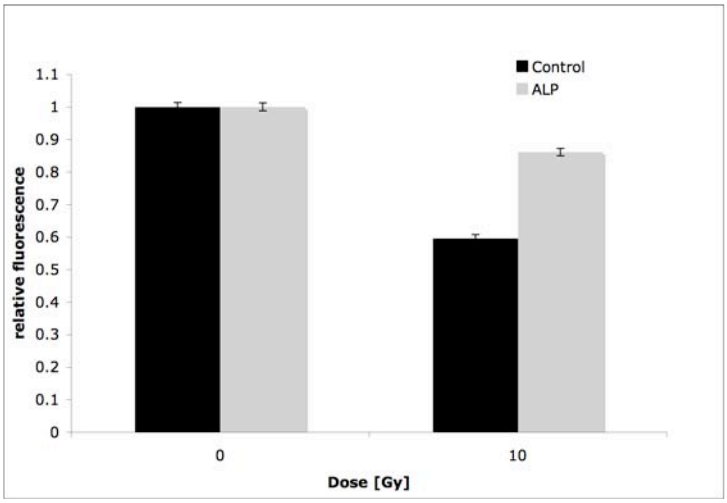

Fig. 3 Radiation-induced proteasome inhibition was prevented by alkaline phosphatase treatment. After irradiation, cell extracts were incubated with alkaline phosphatase at 37 degrees fro 30 minutes. Radiation induced inhibition could be partially reverted by ALP treatment indicating involvement of a kinase activity.

Since the immediate drop in proteasome function indicated posttranslational modifications of the proteasome in response to radiation, we performed simply experiments to test if the proteasome was subject to phosphorylation. As expected, treatment of cells with alkaline phosphatase directly after irradiation restored proteasome function (Figure 3). We hypothesized that most likely candidates for the responsible kinase were located in pathways associated with the EFG receptor, which had already been reported to be activated in response to radiation. In fact, blocking EGFR signaling using a small inhibitor prevented loss of chymotryptic activity in response to radiation (Figure 4). This was

further supported by the novel finding that cells overexpressing the constitutively active form of the EGFR (variant III) were not only protected from radiation-induced proteasome inhibition but instead increased proteasome function after irradiation (Figure 5).

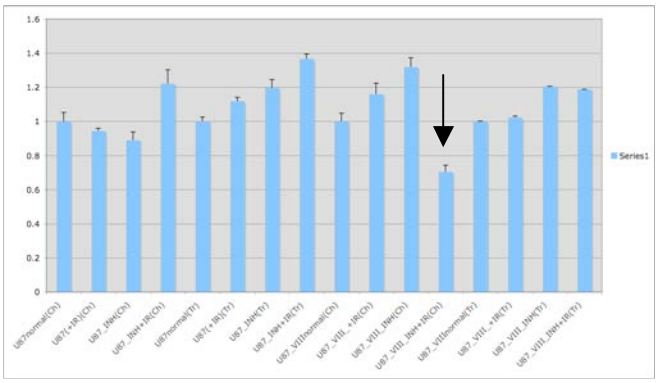

Figure 4. *U87-EGFRvIII proteasome activity. Untreated (1,5,9,13), Plus IR (2,6,10,14), Plus inhibitor (3,7,11,15), inhibitor+IR (4,8,12,16). Chymotrypsin (1-4, 9-12). Trypsin (5-8, 13-16).

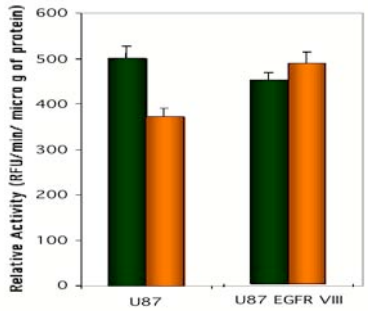

Figure 5 Proteasome function in U87 and U87 EGFRvIII cells after 10Gy irradiation as assessed by fluorogenic assay.

We next sought to optimize the purity of our proteasome preparations to allow a comprehensive analysis of posttranslational modifications of proteasome subunits. In a first attempt, we immuno-precipitated proteasomes form PC-3 cells using an antibody against the 19S regulatory subunit Rpn10. The rationale for this approach was that this would only purify free 19S subunits and 19S subunits bound to 20S core particle but not free 20S proteasomes or immuno-proteasomes, which we had shown, do not react to ionizing radiation with a loss of function. Unfortunately, 1. using SyproRuby as a detection agent, our preparations contained much more protein copurifying with the 26S proteasome than one would expect (Figure 5) and 2., the results varied between the various experiments, indicating loss of structural integrity of the complex with time. Instability of the complex was confirmed in proteasome function assays (Figure 6).

The discrepancy between the number of spots detected in our experiments and data from the literature could be either a technical problem or simply reflect the higher sensitivity of the staining we used in comparison to coomassie blue staining. In order to overcome the shortcomings of glycerol gradient purification on immunoprecipitation we initiated collaboration with Dr. Lan Huang from UC Irvine who provided us with an expression vector for a tagged Rpn11 protein (Rpn11-6xHIS-TEV-Biotin-6xHis). We already produced the retroviral vector and successfully infected PC-3 cell with the construct (Figure 7).

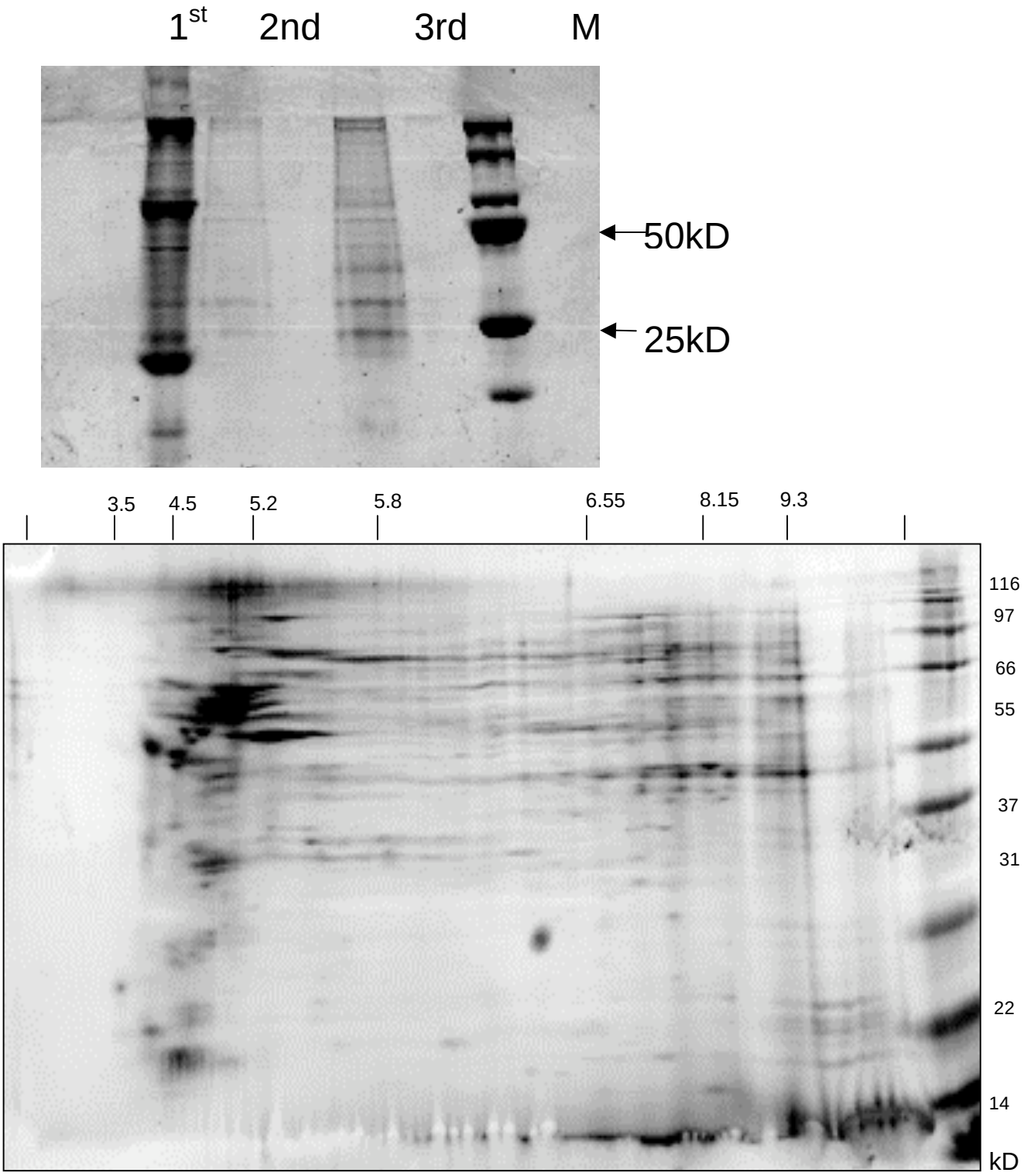

Fig. 6 1D and 2D gel electrophoresis of 26S proteasomes purified by co-immunoprecipitation using an antibody against the 19S subunit Rpn10. The results clearly indicate variability of the cell preparations and coimmunoprecipitation of proteins unrelated to the proteasome.

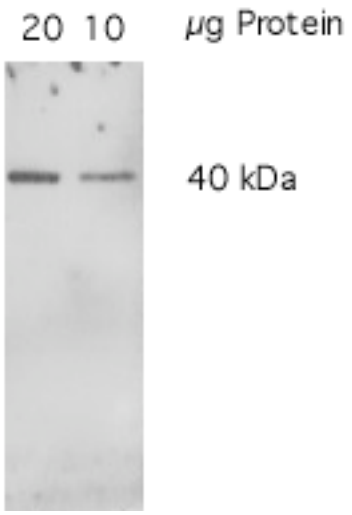

Figure 7 1D gel electrophoresis of immunoprecipitates from cells transfected with an (Rpn11-6xHIS-TEV-Biotin-6xHis). The biotin-his tag bound to beads can be easily removed and the complex can be rapidly analysed by LC-MS/MS.

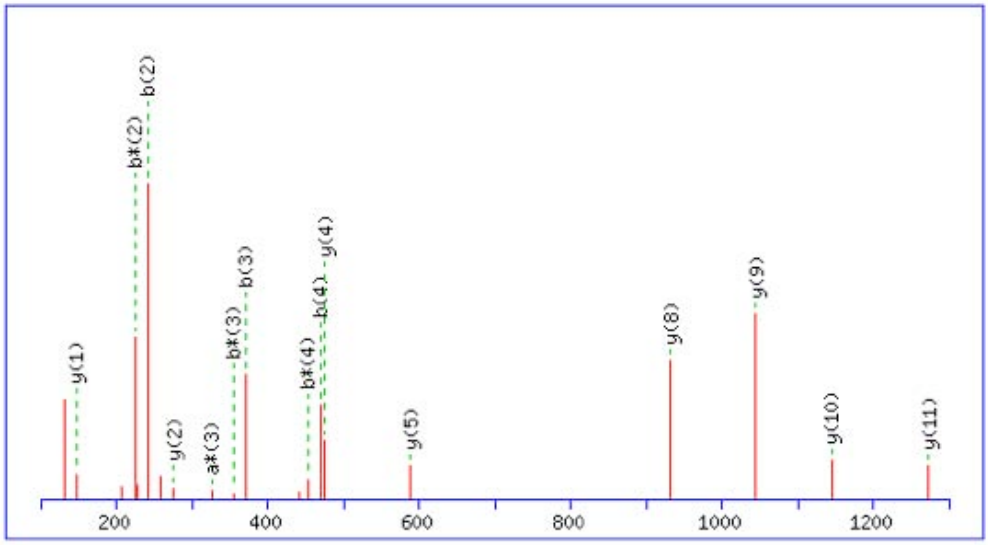

Figure 8. Analysis of 26S proteasomal components at UCLA. The tandem mass spectrum shown identifies the precursor peptide as derived from the 26S proteasome non-ATPase regulatory subunit 12 (human PSD12) with high confidence (Mascot score 76).

Crude cellular extrcts were prepared from human PC-3 cells. Whole cell lysates were irradiated with 10 Gy on ice (control on ice only) and 26S proteasomes were enriched by glycerol gradient fractionation. The protein was precipitated with acetone, dissolved in formic acid and loaded onto a reverse-phase column for analysis by liquid-chromatography with online electrospray-ionization and fraction collection (LC-MS+) providing a first dimension separation of intact proteins. Fractions collected concomitant with the separation were reduced, alkylated and digested with trypsin prior to the second dimension analysis using nano-LC-MSMS. Figure 8 shows the tandem mass spectrum of a peptide analyzed during the nano-LC-MSMS experiment. Collision-activated dissociation yields N-terminal (*b*-ions) and C-terminal (*y*-ions) fragments whose mass is sequence dependent. Proteomics software (Mascot; Matrix Sciences) automatically matched the observed precursor and product masses to a peptide from a known component of the 26S proteasome (PSD 12) with a high confidence score (scores above ~50 are regarded as greater than 95% confident).

This first experiment yielded many other protein identifications in agreement with published work. Electron microscopy confirms radiation-induced changes in these preparations altering, for example, the pore size of certain proteasome-associated structures (see Figure 9).

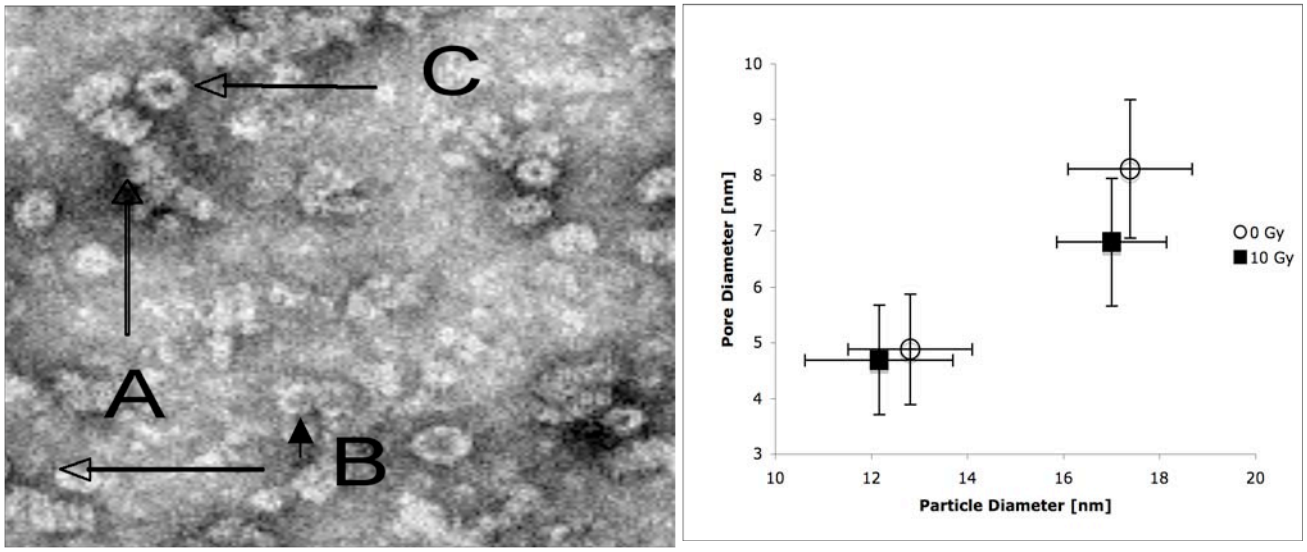

Fig. 9 Left: Negative staining of proteasome preparation in EM showing 26S (A), 20S (B) and putative radiation-altered (C) structures. Right: 10Gy decreases the pore size of C-type, but not B-type, structures.

The experiment described above also yielded intact protein mass spectra as different components eluted from the column. Figure 10 shows the intact protein mass output from LC-MS+ described above. Mass spectra are recorded throughout the chromatogram and individual protein mass spectra appear as they elute from the column, and can be correlated with the protein identifications achieved in the bottom-up proteomics experiments described above. In this way the 58 kDa protein shown was identified as TCP1-eta, annotated as a component of the GroL chaperonin. This protein was only seen in the radiation-treated sample suggesting that it has associated with the 26S proteasome. Although it has to be confirmed, C-type structures in Figure 9 are of the correct morphology to be GroL chaperonin. These experiments highlight the importance of affinity purification of material as described by our collaborator, Dr. Lan Huang, as well as the quantitative proteomics technologies described. While the data are very preliminary, they serve to show our ability to detect what may be important alterations in the proteasome and interacting structures.

The value of the intact mass measurement is illustrated by the fact that the observed mass of the native protein suggests mis-annotation of the stop codon at residue 543 of the human sequence as most other mammals terminate around 530. The calculated mass for residues 1-529 is 57925 Da with measured masses for the mature protein in the range 57938 – 58052 Da. The observed heterogeneity suggests further post-translational modification of the protein, though at this point it is impossible to determine whether this was related to radiation treatment because we did not see this protein in the control sample.

Intact mass protein mass measurements typically provide complementary information to bottom-up peptide based proteomics experiments, helping to keep track of regions of the protein that yield peptides of low recovery efficiency that are not seen in bottom-up experiments, for example.

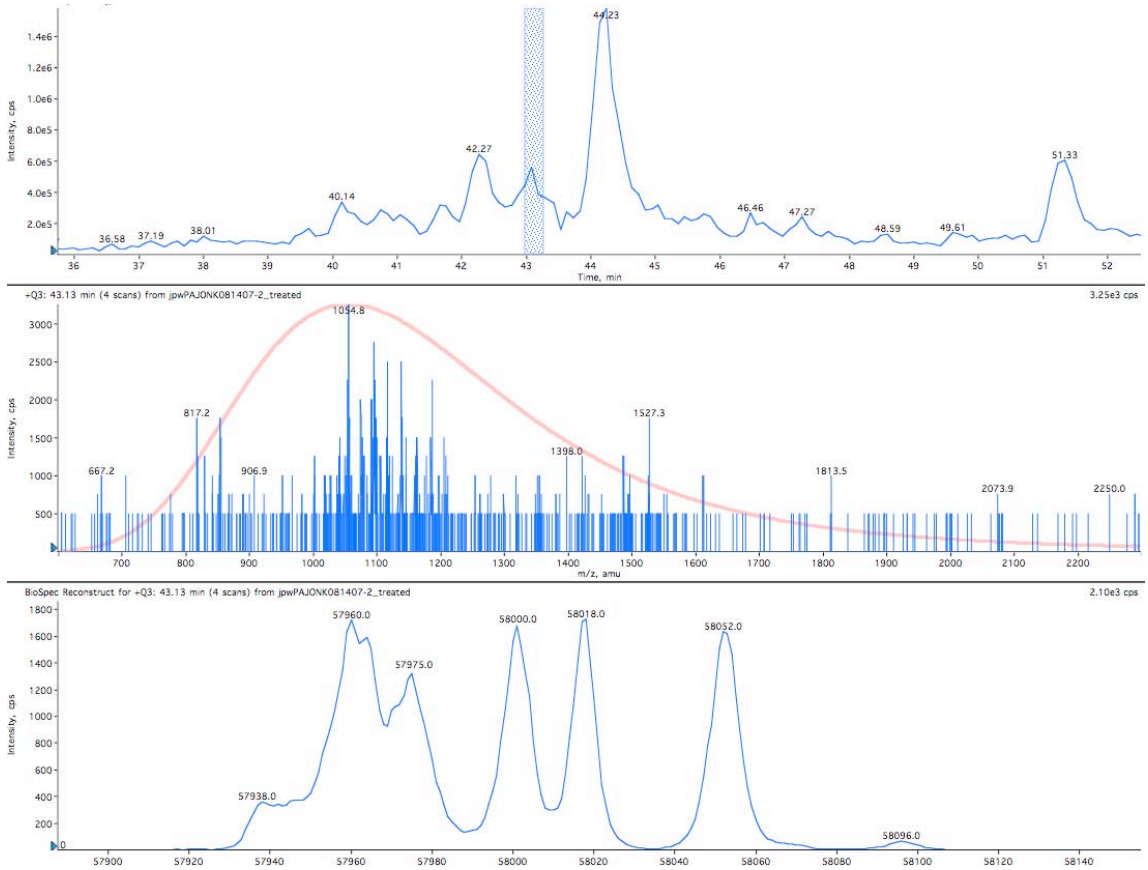

Figure 10. Intact protein mass measurements of human 26S proteasomal components. Electrospray-ionization mass spectrometry was performed every 6 seconds generating an ion chromatogram (top panel) to complement the UV chromatogram (not shown). The mass spectrum recorded in the shaded part of the chromatogram is shown in the center panel showing the multiply charged ions characteristic of this ionization mode. Software (BioMultiView) was used to deconvolute a zero-charge molecular mass profile of the intact protein (lower panel). This protein, chaperonin TCP1-eta subunit, is clearly heterogenous. The mass calculated for residues 1-529 is 57925 Da suggesting removal of C-terminal amino acids as suggested from BLAST comparisons with other mammals.

Key Research Accomplishments

1. Study of the first 9 proteasome sunubits in response to radiation
2. Identification of a first candidate posttranslational modification (phosphorylation)
3. Establishment of prostate cancer cells stably expressing a His-Biotin-tagged Rpn11 subunit to pull down proteasomes and analyze them by mass-spec.
4. Identification the chaperonin TCP1 as a possible novel PIP found after irradiation.

Reportable outcomes

N/A

Conclusions

This year has mainly been spent to set up our systems. The novel findings (chaperonin TCP1 as a binding partner in response to radiation) will be confirmed using a refined a rapid proteomics technique in the next year.

References

N/A

Appendices

N/A